

USAFSAM-TR-88-24

# ADDITIVITY OF RETINAL DAMAGE FOR MULTIPLE-PULSE LASER EXPOSURES

Joseph A. Zuclich, Ph.D.  
Michael F. Blankenstein, M.S.

KRUG International  
Technology Services Division  
406 Breesport  
San Antonio, TX 78216

December 1988

DTIC  
ELECTE  
S APR 1 1989 D  
H

Final Report for Period October 1985 - January 1988

Approved for public release; distribution is unlimited.

Prepared for  
USAF SCHOOL OF AEROSPACE MEDICINE  
Human Systems Division (AFSC)  
Brooks Air Force Base, TX 78235-5301



89 4 094

AD-A206 514

## NOTICES

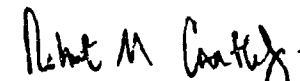
This final report was submitted by KRUG International, Technology Services Division, 406 Breesport, San Antonio, Texas, under contract F33615-84-C-0600, job order 7757-02-82, with the USAF School of Aerospace Medicine, Human Systems Division, AFSC, Brooks Air Force Base, Texas. Lieutenant Colonel Robert M. Cartledge (USAFSAM/RZV) was the Laboratory Project Scientist-in-Charge.

When Government drawings, specifications, or other data are used for any purpose other than in connection with a definitely Government-related procurement, the United States Government incurs no responsibility nor any obligation whatsoever. The fact that the Government may have formulated or in any way supplied the said drawings, specifications, or other data, is not to be regarded by implication, or otherwise in any manner construed, as licensing the holder, or any other person or corporation; or as conveying any rights or permission to manufacture, use, or sell any patented invention that may in any way be related thereto.

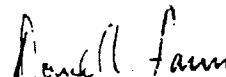
The animals involved in this study were procured, maintained, and used in accordance with the Animal Welfare Act and the "Guide for the Care and Use of Laboratory Animals" prepared by the Institute of Laboratory Animal Resources - National Research Council.

The Office of Public Affairs has reviewed this report, and it is releasable to the National Technical Information Service, where it will be available to the general public, including foreign nationals.

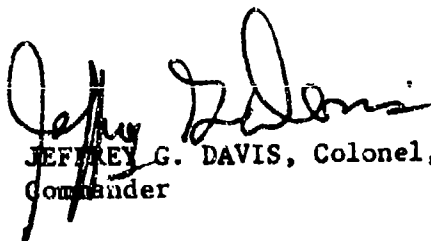
This report has been reviewed and is approved for publication.



ROBERT M. CARTLEDGE, Lt Col, USAF, BSC  
Project Scientist



DONALD N. FARRER, Ph.D.  
Supervisor



JEFFREY G. DAVIS, Colonel, USAF, MC  
Commander

## REPORT DOCUMENTATION PAGE

Form Approved  
OMB No 0704-0188

1a. REPORT SECURITY CLASSIFICATION Unclassified			1b. RESTRICTIVE MARKINGS		
2a. SECURITY CLASSIFICATION AUTHORITY			3. DISTRIBUTION/AVAILABILITY OF REPORT Approved for public release; distribution is unlimited.		
2b. DECLASSIFICATION/DOWNGRADING SCHEDULE			5. MONITORING ORGANIZATION REPORT NUMBER(S) USAFSAM-TR-88-24		
4. PERFORMING ORGANIZATION REPORT NUMBER(S)			7a. NAME OF MONITORING ORGANIZATION USAF School of Aerospace Medicine (RZV)		
6a. NAME OF PERFORMING ORGANIZATION KRUG International Technology Services Division		6b. OFFICE SYMBOL (if applicable)	7b. ADDRESS (City, State, and ZIP Code) Human Systems Division (AFSC) Brooks Air Force Base, TX 78235-5301		
6c. ADDRESS (City, State, and ZIP Code) 406 Breesport San Antonio, TX 78216		9. PROCUREMENT INSTRUMENT IDENTIFICATION NUMBER F33615-84-C-0600			
8a. NAME OF FUNDING/SPONSORING ORGANIZATION		8b. OFFICE SYMBOL (if applicable)	10. SOURCE OF FUNDING NUMBERS		
8c. ADDRESS (City, State, and ZIP Code)		PROGRAM ELEMENT NO 02202F	PROJECT NO 7757	TASK NO 02	WORK UNIT ACCESSION NO 82
11. TITLE (Include Security Classification) Additivity of Retinal Damage for Multiple-Pulse Laser Exposures					
12. PERSONAL AUTHOR(S) Zulich, Joseph A.; and Blankenstein, Michael F.					
13a. TYPE OF REPORT Final		13b. TIME COVERED FROM 85/10 TO 88/01		14. DATE OF REPORT (Year, Month, Day) 1988 December	
15. PAGE COUNT 25					
16. SUPPLEMENTARY NOTATION RZV Protocol Nos 85-02 and 86-07					
17. COSATI CODES			18. SUBJECT TERMS (Continue on reverse if necessary and identify by block number)		
FIELD	GROUP	SUB-GROUP	Additive effects; laser; multiple pulse; ocular damage; retina; thermal mechanism		
09	03				
06	07				
19. ABSTRACT (Continue on reverse if necessary and identify by block number) This study has examined the cumulative effects of multiple-pulse laser exposures in contributing to retinal damage via a thermal mechanism. Three sets of experiments have been conducted to determine the variation of multiple-pulse thresholds: with the interval between pulses; with the number of pulses in the pulse train when the interpulse interval is held constant; and with the retinal image size when both number of pulses and interpulse interval are invariant. In addition, thermal model calculations were carried out to compare model predictions with the experimental data. Conclusions from the experimental data are: (1) The threshold for a multiple-pulse train is related to that for an individual pulse in the train by a function of the number of pulses, but is independent of pulse-repetition frequency and pulse train length. This observation is in general accordance both with the thermal model predictions and with previously proposed empirical models. (Cont'd. on p. ii)					
20. DISTRIBUTION/AVAILABILITY OF ABSTRACT <input checked="" type="checkbox"/> UNCLASSIFIED UNLIMITED <input type="checkbox"/> SAME AS RPT <input type="checkbox"/> DTIC USERS			21. ABSTRACT SECURITY CLASSIFICATION Unclassified		
22a. NAME OF RESPONSIBLE INDIVIDUAL Robert M. Cartledge, Lt Col, USAF, BSC			22b. TELEPHONE (Include Area Code) (512) 536-3622		22c. OFFICE SYMBOL USAFSAM/RZV

(2) The additivity of multiple pulses is quantitatively similar for collimated and expanded laser beams incident at the eye.

(3) The repair or recovery of laser-induced reversible retinal damage (i.e., sub-threshold with respect to the ophthalmoscopic lesion endpoint) is slow, having a time constant of the order of days. Thus, the cumulative nature of multiple-pulse or repeated exposures within a 24-hr period is relatively unaffected by the ongoing repair process; and only when repeated daily exposures are of concern does the repair process become a factor. *K. J. V. J.*

Keywords.

Laser damage; retina; (KT) ~~at~~

4  
CHURCH  
1880

Accession For	
NTIS GRANT	<input checked="" type="checkbox"/>
DTIC TAB	<input type="checkbox"/>
Unannounced	<input type="checkbox"/>
Justification	
By	
Distribution/	
Availability Codes	
Dist	Avail and/or Special
A-1	

## TABLE OF CONTENTS

	<u>Page</u>
ACKNOWLEDGMENTS. . . . .	iv
INTRODUCTION . . . . .	1
Military Relevancy . . . . .	1
Background . . . . .	1
METHOD . . . . .	3
Subjects . . . . .	3
Apparatus . . . . .	4
Laser Exposures . . . . .	4
Data Analysis . . . . .	5
Thermal Model Calculations . . . . .	5
RESULTS . . . . .	6
DISCUSSION . . . . .	8
Experimental Data . . . . .	8
Thermal Model--Empirical Model--Experimental Data Comparisons . . .	12
REFERENCES . . . . .	17

## Figures

Fig.  
No.

1.	Log-log plot of threshold vs. number of pulses . . . . .	10
2.	Retinal threshold as a function of retinal image diameter of the laser beam . . . . .	11
3.	Log-log plot of predicted retinal threshold vs. pulsewidth . .	13
4.	Log-log plot of threshold vs. number of pulses for 40- $\mu$ s, 647-nm krypton laser radiation at high PRFs . . . . .	16

(Cont'd. on next page)

## Tables

<u>Table No.</u>		<u>Page</u>
1.	Retinal thresholds for two 100-ms pulses of 647-nm krypton laser radiation . . . . .	6
2.	Retinal thresholds for 100-ms pulse trains of 647-nm krypton laser radiation . . . . .	7
3.	Retinal thresholds for 100-ms pulses of 647-nm krypton laser radiation as a function of retinal image diameter . . . . .	8
4.	Relative retinal thresholds for trains of 100-ms, 647-nm krypton laser pulses . . . . .	14

## ACKNOWLEDGMENTS

Technical and engineering support for the experimental parts of this study were provided, respectively, by Messrs. Douglas J. Coffey and Anthony J. Catalano (of KRUG International). Drs. Mary Morton-Gibson (a participant in the USAF Summer Faculty Research Program) and Fred Loxsom (a consultant from the Physics Department, Trinity University, San Antonio) were responsible for modifications of the thermal model program which allowed the authors to complete the calculations reported herein.

# ADDITIVITY OF RETINAL DAMAGE FOR MULTIPLE-PULSE LASER EXPOSURES

## INTRODUCTION

### Military Relevancy

The ever-increasing use of lasers in military, medical, and industrial environments presages increasing incidents of personnel exposed to harmful levels of laser radiation. While a broad data base, accumulated over the past two decades, defines ocular damage thresholds for single-pulse exposures from either continuous-wave (cw) or pulsed sources, relatively few studies have examined the effects of multiple-pulse or repeated exposures. However, a field scenario can easily be envisioned in which the dynamics of laser beams and targets, both in motion, dictate that a sequence of exposures is as likely as--or more likely than--a single-exposure episode. If a repetitively pulsed laser is involved with a pulse-repetition frequency greater than 10 Hz (up to megahertz), a few or many pulses may strike the retina with each exposure encounter. Because of the task or mission at hand, the targeted or accidentally exposed personnel could have a tendency (if not a compelling reason) to look in the direction from which the laser beam emanates, so that areas of exposed retinal tissue could be concentrated in the macular area. Under such a scenario, the probability of a given patch of retinal tissue receiving multiple exposures might be considerable, and would increase with the time that personnel remained vulnerable to laser exposures. Thus, in evaluating potential ocular effects of lasers, achieving an understanding of the cumulative effects of repeated exposures is of significance.

### Background

The genesis of thermal damage additivity studies is the work of Henriques (1) and Moritz and Henriques (2). In their studies of thermal injury to skin, they observed additivity of damage from exposures over periods of several hours; and they defined the Henriques damage integral as a measure of extent of damage as a function of the spatial-temporal temperature increases associated with a thermal insult. The Henriques damage integral has been incorporated into thermal models of laser-induced ocular damage developed by Mainster et al. (3) and Takata et al. (4). The model of Takata et al. has been tested against experimental thresholds for ophthalmoscopically visible lesions induced by single-pulse laser exposures, and has proved to be a highly reliable predictor of retinal damage threshold for pulsewidths ranging from  $10^{-7}$  to  $10^3$  s (4). For multiple-pulse exposures, the thermal model was not tested in any systematic manner.

The need for further quantitative studies of the additive effects of multiple-pulse exposures is perhaps best illustrated by examining the treatment of multiple pulses in existing laser safety standards. The current Air Force Occupational Safety and Health (AFOSH) standard (5) treats pulses separated by  $\geq 1$  s as totally independent events (i.e., zero additivity). The American National Standards Institute's (ANSI) Standard for the Safe Use of Lasers, prior to a 1986 revision, required that pulses at repetition rates of  $< 1$  Hz be added over a 24-hr period (i.e., total additivity) (6). The revised ANSI standard (7) defines multiple-pulse exposures only for cases with a pulse repetition frequency (PRF)  $> 1$  Hz and thus, by omission, leaves exposures separated by  $\geq 1$  s to be treated as independent single-pulse events. While the old ANSI position of total additivity over a 24-hr period may have been unnecessarily conservative, the current ANSI and AFOSH treatments--with no additivity for exposures separated by more than 1 s--may be inadequate, in some cases, for defining suitable protection from multiple-pulse exposures.

The most recent revision of the ANSI laser safety standard suggests an empirically derived treatment for multiple-pulse exposures (7). According to the standard, the maximum permissible exposure (MPE) per pulse for a train of  $n$  identical pulses is equal to  $(n)^{-1/4}$  times the MPE for a single pulse in the train. This simple and totally empirical relationship provides an acceptable approximation to the body of multiple-pulse threshold data which existed at the time this relationship was first proposed (8,9). Obviously, one must use great caution in generally applying a relationship which depends on only the one exposure parameter ( $n$ ), and which has not been systematically tested (because of a lack of experimental data), versus wide ranges of other exposure parameters (e.g., PRF, pulse train length, beam divergence, etc.).

The objective of the current work is to provide a quantitative basis for evaluating the cumulative nature of multiple-pulse or repeated exposures for the various exposure conditions which may be anticipated with existing laser systems. In particular, this work is concerned with additivity of repeated subthreshold laser exposures, where the exposure conditions are such that any resultant retinal lesion would arise from a thermal damage mechanism. Therefore, this work encompasses very broad ranges of exposure parameters, but excludes long exposures ( $> 1$  s) to short visible or ultraviolet wavelengths where photochemical processes might result in retinal damage at exposure levels insufficient to induce thermal damage (10). Also excluded are ultra-short pulsewidth exposures (of a nanosecond or less) where photo-acoustic and other non-linear mechanisms may be dominant (11).

Two basic tissue rate processes must be considered in assessing the additivity of repeated pulses. The first is the thermal conductivity of the tissue. For the retina, thermal relaxation times are on the order of milliseconds (12). The second rate process is that of tissue repair of reversible damage. The existence of a repair process is an a priori assumption based on observations that repeated low-level exposures (e.g., ambient sunlight) are not cumulative over indefinite periods of time, or we would all suffer severe retinal degeneration in short order. Studies in this laboratory have quantitatively assessed corneal and retinal repair



rates following ultraviolet and blue-light exposures (where photochemical damage mechanisms are involved). The time constants associated with tissue repair were found to be approximately 2 and 4 days for the cornea and retina, respectively (13,14). That a comparable repair rate exists after laser-induced thermal insult to the retina is uncertain. However, the organism's response may be determined by the given degree of tissue damage, without regard to (or "memory" of) the exposure parameters and specific mechanism which induced that degree of damage.

Given the two tissue rate processes just discussed, considerations of multiple-pulse laser exposures may relate to the relative values of the time constants associated with these rate processes on the one hand, and with the pulsewidth, PRF, and pulse train length on the other hand. Thus, for PRFs  $\gg 1$  Hz, thermal relaxation of the exposed area may not be completed during the interval between pulses; and the consequences of repeated pulses may be additive in a manner consistent with the higher and higher peak temperatures achieved with each successive pulse. A different result may be achieved if the identical sequence of pulses is delivered over a longer time frame (with PRF  $\leq 1$  Hz) where thermal relaxation is effectively completed during each inter-pulse interval. In such a case, the peak temperature at any point never exceeds that resulting from a single pulse in the train.

Regardless of PRF, if one is concerned with evaluating the cumulative effects over periods of time comparable to or longer than the tissue repair rate, then the additivity of repeated exposures is diminished by the ongoing repair process. Only when the pulse train length is much less than the tissue repair rate can the latter be ignored in calculating the net cumulative effect.

Ultimately then, we seek a quantitative basis for evaluating the additive nature of multiple-pulse or repeated exposures for the various contingencies just mentioned; i.e., for PRFs ranging from much less than to much greater than the thermal relaxation rate, and for pulse train lengths ranging from much less than to much greater than the tissue repair rate.

## METHOD

### Subjects

Experimental subjects were rhesus monkeys (*Macaca mulatta*). Potential subjects were screened with a slit lamp and fundus camera, and only animals with clear ocular media and normal fundi were used. In addition, no animal was used that had a refractive error difference of more than 0.50 diopter in any meridian.

One day before a planned experiment, 2-3 drops of atropine sulfate (1% ophthalmic solution) were introduced into each conjunctival sac to induce cycloplegia. The animals were tranquilized with an injection of ketamine hydrochloride (12-14 mg/kg body weight, i.m.), and anesthetized to effect with sodium pentobarbital introduced through a catheter in a superficial leg

vein. Throughout the experiments, the primate core temperature was monitored by means of a rectal probe, and maintained at  $37 \pm 1^\circ\text{C}$  by means of a thermal blanket.

### Apparatus

All exposures were carried out with a Spectra Physics 171 krypton laser with a cw output at 647 nm. An electronically controlled mechanical shutter and two Vincent Associates shutter drive timers in series provided a programmable means of choosing the pulsewidth, pulse repetition rate, and pulse-train duration. In all cases, a 100-ms pulsewidth was chosen, but the PRF and pulse train length were varied.

A pellicle beamsplitter was positioned to deflect a fraction of the shuttered beam to a silicon photodiode detector and Photodyne 66XLA optical power-energy meter. In the power mode and with the shutter open, this meter monitored the cw output of the laser before and after each exposure. In the energy mode, the meter measured the total energy delivered in each shuttered pulse train. In either case, the relative numbers obtained from the deflected portion of the beam were converted to absolute levels, incident at the subject's cornea, by cross-calibrating against a second photodiode detector-Photodyne meter combination where the second detector was inserted at the position otherwise occupied by the subject. The cross-calibration was completed before and after each exposure session.

A Zeiss fundus camera was fitted with a swing-out mirror which, when out of position, allowed fundus camera viewing of the subject's retina. When in position, the mirror deflected the incoming laser beam through the subject's pupil and in the direction collinear with the optic axis of the fundus camera, thus allowing the beam to be steered to a pre-selected spot on the fundus according to the positioning of the subject.

The krypton laser beam had a divergence of 1 mrad and a diameter of  $\sim 2$  mm when incident at the corneal plane. To vary the retinal image size of the beam, an ophthalmic trial lens was placed in the beam path at a point 6 in. from the corneal plane. For example, a +7 diopter lens at this position yielded a  $200\text{-}\mu\text{m}$  retinal image diameter. This was verified by direct observation with the fundus camera when a pellicle beamsplitter replaced the swing-out mirror to permit fundus viewing during low-level laser exposure, thus allowing the retinal image to be measured by a calibrated reticle incorporated into the fundus camera optics. When no trial lens was used and the collimated laser beam was allowed through the pupil, the retinal image diameter was  $\sim 30\text{ }\mu\text{m}$ .

### Laser Exposures

Anesthetized animals were mounted on an adjustable stage in front of the fundus camera, and their eyes were positioned by translational and rotational stage adjustments. At the beginning of each exposure session,

extramacular marker lesions were placed in each eye to define a 3 x 3 macular grid for placement of experimental exposures. Marker lesions were generated by single 100-ms pulses, by using the collimated 647-nm laser beam with an energy of 8 to 10 mJ. Marker lesions, although initially punctate, typically developed to ~100- $\mu$ m diameter within 1 hr postexposure.

After the marker lesions developed, macular exposures were delivered to each of the nine marker grid sites. The range of doses was from ~0.5 to 2.0 times the estimated threshold for an ophthalmoscopically visible lesion. For the set of exposures delivered to any given eye, only the power of the laser was varied, while all other exposure parameters were held constant. Exposures were generally completed for both eyes during a single experimental session. The animal was maintained at an even plane of anesthesia until the lesion-no lesion ophthalmoscopic readings were completed at 1 hr postexposure.

### Data Analysis

The lesion-no lesion data were subsequently analyzed by the method of probit analysis (15). Generally, data from six eyes (up to 54 data points) were used for each threshold determination. A probit program was used to calculate the dose at which there is a 50% probability of inducing damage (ED<sub>50</sub>) and the requested confidence limits (usually 95%) on the ED<sub>50</sub>. The program also generates a probability vs. dose curve, so that other thresholds (e.g., ED<sub>10</sub> and ED<sub>90</sub>) are available as desired.

### Thermal Model Calculations

A retinal thermal model was used to predict damage thresholds for comparison with the experimentally determined multiple-pulse thresholds and with the empirical fits of multiple-pulse threshold data (8,9). The model, initially developed by Takata et al. (4), has been modified to handle the multiple-pulse cases of interest here and to run on a Digital Equipment Corporation microVAX II computer.

The model is divided into two parts--one that computes the laser-induced temperature increases in the eye (for spatial coordinates and as a function of time); and a second that uses the predicted temperature increases to determine the degree and extent of irreversible tissue damage. The mathematical basis for the temperature predictions is the standard heat-conduction equation in cylindrical coordinates. The technique used is to approximate the heat conduction equation by a grid of finite difference equations, and solve these at successive times by using the numerical solution developed by Peaceman and Rachford (16). Since the resulting equations are linear, temperature rises due to multiple pulses can be predicted by adding the temperature increments due to individual pulses with the appropriate temporal offset.

The time-temperature history predictions are then fed to the second part of the model, which applies the Henriques damage criteria to determine the extent of irreversible tissue damage, if any.

Appropriate values for reflectivities, transmissivities, and absorptivities for each ocular component--as well as geometric data and indices of refraction for the rhesus monkey and human eyes--have been tabulated (4,17) and are used for the current model calculations.

## RESULTS

The ophthalmoscopic lesion threshold was first determined for single 100-ms, 647-nm pulses from the krypton laser. After this baseline determination, thresholds were determined for two identical 100-ms pulses with varying times between exposures. The threshold for two pulses separated by 0.01 s represented the shortest inter-pulse interval which could be accurately obtained with the mechanical shutters used. Other inter-pulse intervals were 0.06 s, 0.6 s, 6.0 s, 60 s, and 600 s (10 min). The  $ED_{50}$  values and confidence limits for this series of experiments are listed in Table 1. ( $ED_{50}$  is used to designate the threshold for a train of  $n$  pulses in terms of total energy delivered by the pulse train.)

TABLE 1. RETINAL THRESHOLDS FOR TWO 100-ms PULSES OF 647-nm KRYPTON LASER RADIATION(a)

Pulse separation (s)	$ED_{50}^2$ (b) (mJ)	95% confidence intervals (mJ)
0(c)	2.6(c)	2.3 - 2.8
0.01	5.0	3.6 - 6.4
0.06	4.3	3.9 - 5.2
0.6	4.6	4.2 - 5.1
6.0	4.5	3.0 - 6.7
60	4.1	3.7 - 4.4
600	4.4	4.0 - 5.0
--	4.5(d)	4.2 - 4.8(d)

(a) 200- $\mu$ m retinal image diameter

(b) Total energy, two pulses

(c) Single-pulse threshold,  $ED_{50}$

(d) Calculated by pooling all two-pulse threshold data.

A second series of experiments was conducted leaving the interpulse interval fixed at 0.06 s (6.25 Hz PRF) and varying the number of pulses. The results are presented in Table 2.

TABLE 2. RETINAL THRESHOLDS FOR 100-ms PULSE TRAINS OF 647-nm KRYPTON LASER RADIATION (a)

Number of pulses (n)	ED <sub>50</sub> <sup>n</sup> (mJ)	95% confidence intervals (mJ)	ED <sub>50</sub> <sup>n</sup> /pulse (mJ)
1(b)	2.6(b)	2.3 - 2.8	2.6
2	4.3	3.9 - 5.2	2.2
10	20	17 - 21	2.0
50	87	82 - 91	1.7

(a) 200- $\mu$ m retinal image diameter, 6.25 Hz PRF

(b) Single-pulse threshold, ED<sub>50</sub>.

All of the foregoing data were generated by using a 200- $\mu$ m retinal image diameter of the laser beam. This expanded image size was chosen to insure that individual pulses in a multiple-pulse sequence could accurately be delivered to irradiate the chosen patch of retinal tissue. In order to examine the dependence of multiple-pulse additivity on retinal image size, the threshold determination for two 647-nm, 100-ms pulses, at 6.25 Hz PRF, was repeated for ~30- $\mu$ m and 500- $\mu$ m retinal image diameters. The 30- $\mu$ m diameter was obtained when the collimated laser beam was incident at the cornea.

The grid of macular exposure sites was adjusted according to the retinal spot size to avoid overlapping of adjacent grid sites. Thus, 2 x 2 grids were used for the case of 500- $\mu$ m retinal image diameter, as opposed to 3 x 3 grids for the 200- $\mu$ m case, and 4 x 4 grids for the 30- $\mu$ m spot sizes. For the 500- $\mu$ m case only, 4-6 additional exposures per eye were delivered to areas just adjacent to the macula, so that the probit calculations could be based on a comparable number of data points for each case. No significant difference was found between the macular ED<sub>50</sub> threshold and the paramacular ED<sub>50</sub> for either the single-pulse or the double-pulse exposures; and only the combined probit results (macular plus paramacular) are shown in Table 3.

For each of the three retinal image sizes, the single-pulse threshold was first determined for comparison to the corresponding two-pulse threshold (Table 3).

TABLE 3. RETINAL THRESHOLDS FOR 100-ms PULSES OF 647-nm KRYPTON LASER RADIATION AS A FUNCTION OF RETINAL IMAGE DIAMETER

Retinal image diameter ( $\mu\text{m}$ )	Single-pulse threshold		Two-pulse threshold(a)	
	ED <sub>50</sub> <sup>1</sup> (mJ)	95% confidence intervals (mJ)	ED <sub>50</sub> <sup>2</sup> (mJ)	95% confidence intervals (mJ)
30	1.0	0.7 - 1.2	2.3	1.9 - 2.7
200	2.6	2.3 - 2.8	4.3	3.9 - 5.2
500	6.0(b)	5.6 - 6.6	9.7(b)	8.5 - 10.6

(a) 6.25 Hz PRF

(b) Calculated by pooling macular and paramacular exposure data; all other thresholds based on macular data only.

## DISCUSSION

### Experimental Data

The data of Table 1 indicate that the degree of additivity for two pulses remains approximately constant as the time between exposures is varied over several orders of magnitude from 0.01 s to 10 min. When the two pulses are separated by  $>1$  s, thermal equilibrium is certainly reached before the second pulse is delivered. On the other hand, for pulses separated by only 0.01 s or 0.06 s, the irradiated tissue is still at an elevated temperature induced by the first pulse when the second pulse is delivered. According to our thermal model calculations (discussed in the next section), the temperature at or near the center of the irradiated area, at 0.01 s after the initial exposure, has relaxed to roughly half of the peak temperature increment achieved at the end of that first pulse; and, at 0.06 s, the temperature has relaxed to  $\sim 10\%$  of the peak value. Nevertheless, as indicated in Table 1, the additivity of the two pulses is independent of whether or not thermal relaxation is completed during the interpulse interval. The agreement of the thermal model predictions with this observation provides tentative validation of the numerical solution technique used in the thermal model (4,16).

This result appears also to support the simple empirical model that the threshold per pulse for a train of  $n$  identical pulses is related to the threshold for a single pulse from that train by the factor  $n^{-1/4}$ , and is independent of PRF or total train length. For  $n = 2$ , the  $n^{-1/4}$  factor indicates that the threshold per pulse is 0.84 times the single-pulse threshold, thus equating to a predicted ED<sub>50</sub> = 4.4 mJ, as compared with the observed value of 4.5 mJ for the pooled set of all 2-pulse threshold data from Table 1.

A second conclusion to be drawn from the Table 1 data is that any tissue repair process must proceed with a time constant  $\gg 10$  min. We attempted to determine the additivity for two pulses separated by 24 hr, and found a threshold indicating little contribution from a repair process even over this time frame. However, direct comparison of these data with the thresholds listed in Table 1 is confounded by the fact that the single-pulse threshold based on observation of a minimum visible lesion at 24-hr post-exposure is lower than that based on the 1-hr criteria used here (18). Because the majority of published retinal threshold data (for both single-pulse and multiple-pulse exposures) is based on a 1-hr criteria, we did not pursue further the question of pulses separated by  $>1$  hr. Without additional experimental data, we suggest that the retinal repair rate is comparable to the 96-hr time constant reported by Griess and Blankenstein after exposures to 458-nm argon laser radiation (14).

When the data of Table 2 are plotted on a log-log graph of threshold vs. number of pulses (Fig. 1), a linear relationship is found with a slope of 0.91. The accepted empirical relationship (7-9), that the threshold per pulse for a train of  $n$  pulses of pulsewidth  $t$  is equal to  $n^{-1/4}$  times the single-pulse threshold, is equivalent to:

$$ED_{50}^n(t) = n^{3/4} ED_{50}(t), \quad (1)$$

which predicts a slope of 0.75. Using the single-pulse threshold from Table 2 ( $ED_{50} = 2.6$  mJ), the predicted values of  $ED_{50}^n$  were calculated from Equation 1 and plotted on Figure 1 for comparison with the experimental data. (Further comparisons between experimental data, empirical model predictions, and thermal model predictions are included in the next report section.)

The data of Table 3 were collected to assess the relative additivity of repeated exposures to a point source and an extended source. An earlier study on multiple-pulse thresholds from a Q-switched neodymium:yttrium-aluminum-garnet (Nd:YAG) laser (16-ns pulsewidth, 1064-nm wavelength) found no additivity for exposures with a 900- $\mu$ m retinal image diameter (19); but, for collimated beam exposures with the same source, the multiple-pulse threshold followed the empirical model (Eq. 1). We find no trend indicating that the additivity is diminished for larger retinal spot sizes. The relative additivity is shown in Figure 2, where the two-pulse thresholds,  $ED_{50}^2$ , are plotted vs. retinal spot size for comparison to the cases of zero additivity (i.e.,  $ED_{50}^2 = 2 ED_{50}$ ) and total additivity ( $ED_{50}^2 = ED_{50}$ ). Quantitative assessment of additivity for the collimated beam case is problematical in view of the exposure parameters employed in this experiment. With a 100-ms pulsewidth and a 6.25 Hz PRF, the duration of a two-pulse exposure is 260 ms. Eye drifting of sufficient magnitude to cause significant displacement of the exposure site relative to the 30- $\mu$ m retinal image diameter is certainly possible, if not probable, within this time frame; but such eye drifting would be undiscernible by the pre- vs. post-exposure fundus camera observations, unless the drift were  $>50$   $\mu$ m. On the other hand, with a 200  $\mu$ m or larger retinal image diameter, a drift resulting in significant displacement of the exposure sites for two or more pulses would be easily noticeable by fundus camera observation, and would serve as grounds for discarding the data for that exposure.

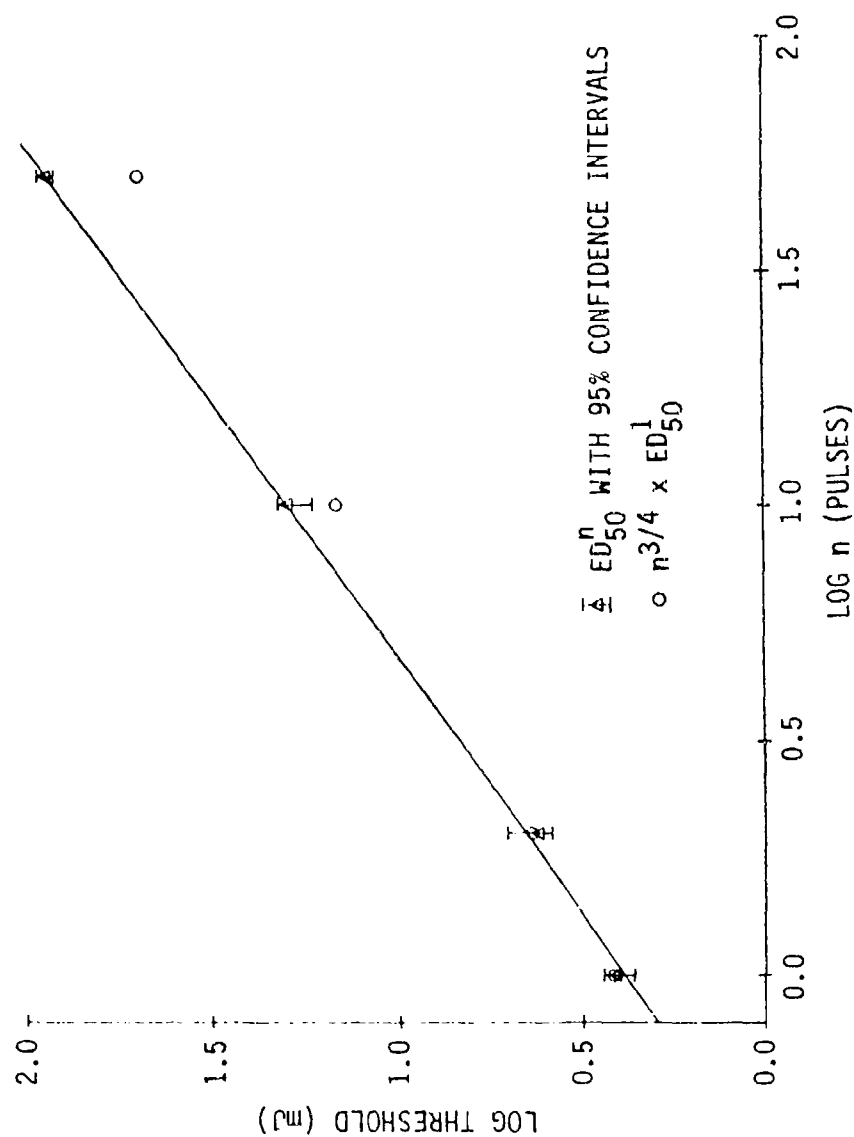


Figure 1. Log-log plot of threshold vs. number of pulses. The  $ED_{50}^n$  thresholds and 95% confidence intervals from Table 2 are plotted and fit (via a least-squares calculation) with a straight line having a slope of 0.91. For comparison, the multiple-pulse thresholds predicted by the empirical model  $ED_{50}^n = n^{3/4} ED_{50}^1$  are also shown.



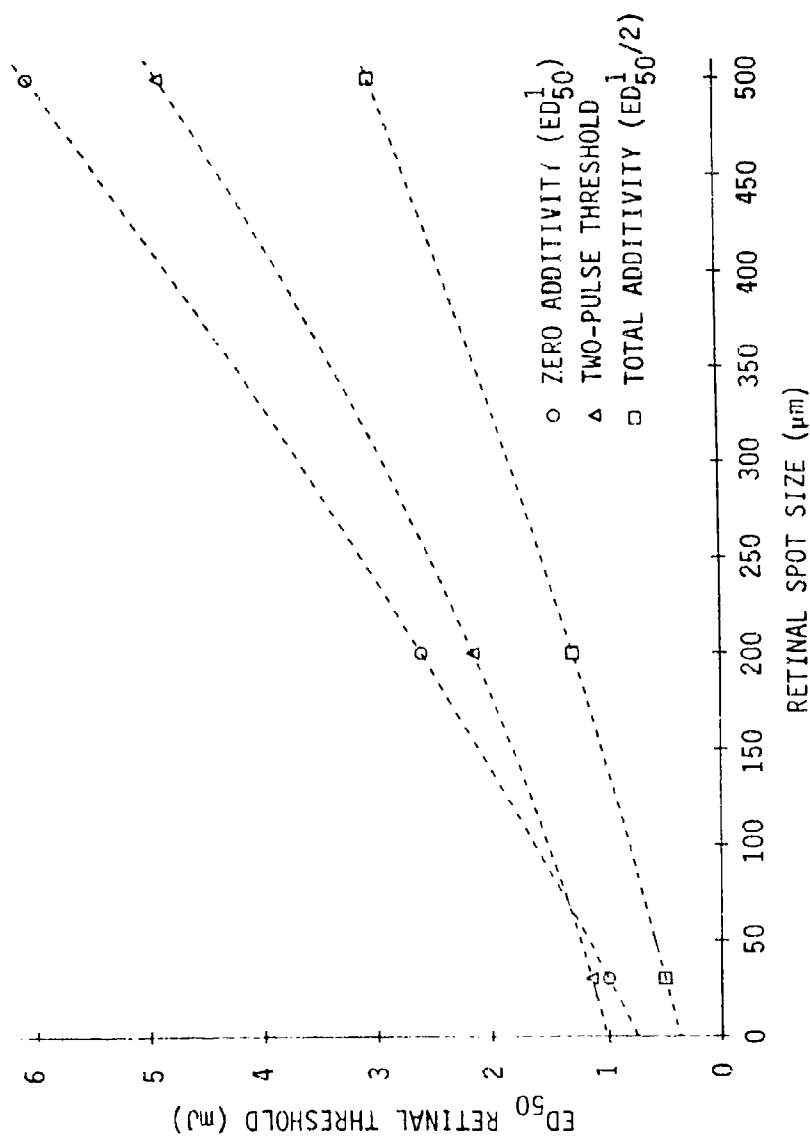


Figure 2. Retinal threshold as a function of retinal image diameter of the laser beam. Both the single-pulse ( $\text{ED}_{50}^1$ ) and two-pulse thresholds ( $\text{ED}_{50}^2/2$ ) from Table 3 are plotted for the three values of retinal image diameter. The curve of  $\text{ED}_{50}^1$  vs. retinal image diameter represents the extreme of zero additivity for the two-pulse exposures. The other extreme (total additivity) is found by plotting  $\text{ED}_{50}^1/2$  vs. retinal image size.

We believe that the apparent discrepancy between our findings and those of Griess et al. (19) may be related to the damage mechanism prevalent with each set of exposures. The exposure parameters for the current work were chosen to minimize the possibility of interference from anything other than a thermal damage mechanism. The Q-switched pulses used by Griess et al. almost certainly infringe upon the regime where photo-acoustic or mechanical shock mechanisms compete with the thermal mechanism; and the shock mechanism may show a greater dominance when larger areas of tissue are irradiated. If so, then the thresholds reported by Griess et al. for 900- $\mu\text{m}$  retinal spot sizes could result from a peak-power dependent mechanism, and would not show additivity of repeated sub-threshold exposures. For the minimal retinal image sizes, however, the thermal mechanism could still be competitive, if not dominant, thus explaining why the multiple-pulse exposures of Griess et al. show additivity comparable to that in other studies (19).

#### Thermal Model---Empirical Model--Experimental Data Comparisons

The discussion of the thermal model predictions of multiple-pulse thresholds must begin with an examination of the behavior of the model in predicting single-pulse thresholds. In fact, the thermal model has been used with great success in predicting retinal thresholds for single laser exposures for wide ranges of laser beam parameters, including pulsewidths from  $10^{-7}$  to  $10^3$  s (4,12). We choose to examine, first, the variation of threshold vs. pulsewidth, according to model predictions compared with the dependence derived from experimental threshold data and used in laser safety standards (5-7). For visible and near-infrared wavelengths, the retinal damage threshold is found to vary as  $t^{3/4}$ , where  $t$  is pulsewidth. This empirical relationship holds over a nominal pulsewidth range from  $1.8 \times 10^{-5}$  s to 10 s (or longer, depending on wavelength). For pulsewidths much less than the thermal relaxation time of the exposed tissue, threshold should be independent of pulsewidth, assuming a thermal damage mechanism.

The threshold vs. pulsewidth behavior has been plotted in Figure 3. The solid line is the MPE for visible wavelengths, according to the ANSI and AFOSH laser safety standards (5-7). As already indicated, the slope of the curve for  $t > 1.8 \times 10^{-5}$  s is equal to 0.75. Thermal model predictions are plotted on the curve for two cases, both of which assume a 647-nm, 2-mm-diameter beam incident at the cornea with a Gaussian profile. In the first case, a 1-mrad beam divergence is specified, and the model uses a point-spread function to calculate the geometrical distribution of light on the retina. (This distribution approximates a Gaussian profile with a  $1/e^2$  diameter of 30  $\mu\text{m}$ .) In the second case, a 200- $\mu\text{m}$  retinal image diameter is specified (the model's point-spread subroutine is bypassed), to match the experimentally chosen retinal image size.

For both the collimated and expanded beams, the thresholds predicted by the thermal model approximate the MPE curve and follow the appropriate linear behavior for pulsewidths either much less than or much greater than the thermal relaxation time. For long pulsewidths, however, the slope for both the collimated and the expanded beam curves approaches ~0.90, compared to the value of 0.75 defined by the safety standards.

Now, having examined the behavior of threshold vs. pulsewidth for single-pulse exposures, we consider the multiple-pulse case. The empirical

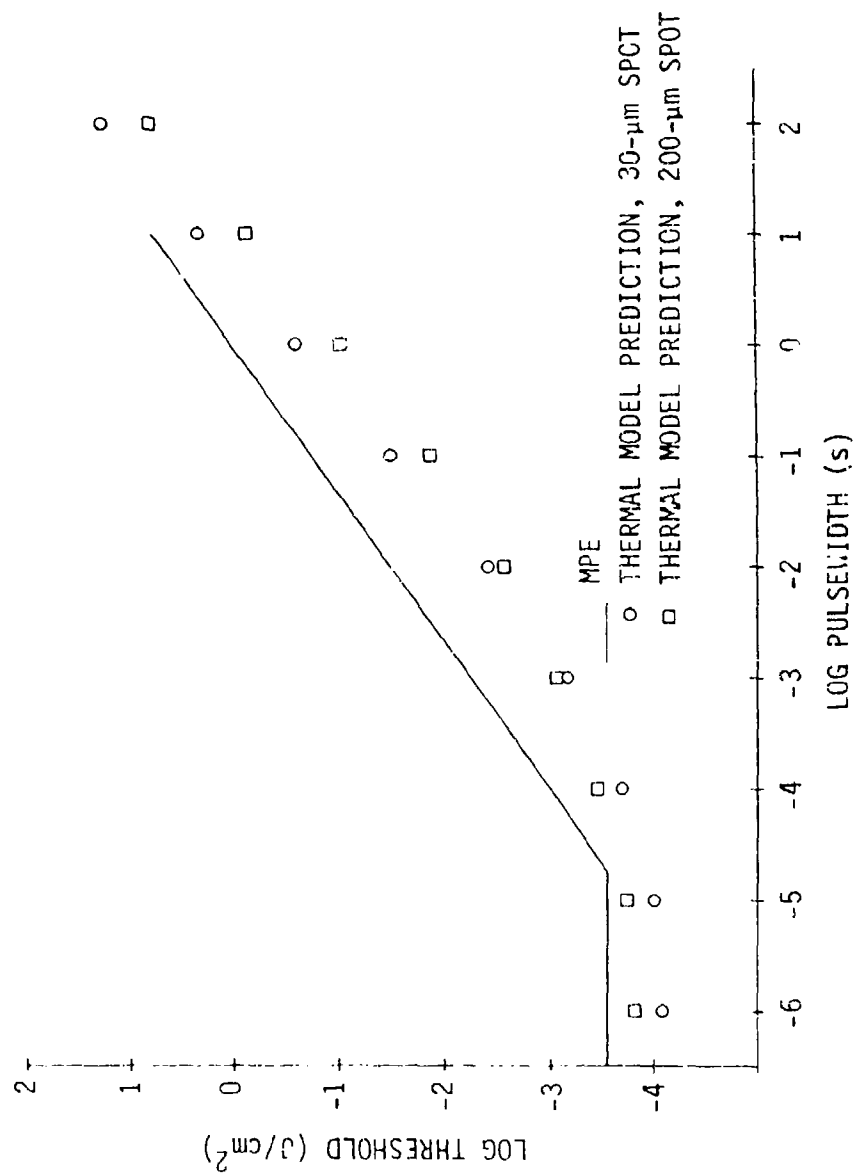


Figure 3. Log-log plot of predicted retinal threshold vs. pulsewidth. Model predictions are shown for both a collimated beam (minimal or 30- $\mu\text{m}$  retinal image diameter) and a diverging beam (200- $\mu\text{m}$  retinal image diameter) incident at the cornea. The solid curve shows the MPE levels according to prevailing laser safety standards (5,7).

model expressed by Equation 1 provides a reasonable fit to published experimental multiple-pulse threshold data (8,9), and has been adopted for the treatment of multiple-pulse exposures in the latest ANSI laser safety standard (7). Since the single-pulse threshold varies as  $(t)^{3/4}$ , Equation 1 is consistent with the case of  $n$  contiguous pulses of pulsewidth,  $t$ . That is, since:

$$ED_{50}^1(t) = c(t)^{3/4}, \quad (2)$$

where  $ED_{50}^1(t)$  is the single-pulse threshold for a pulsewidth,  $t$ , and  $c$  is a constant--then:

$$\begin{aligned} ED_{50}^1(nt) &= c(nt)^{3/4} \\ &= n^{3/4} ED_{50}^1(t). \end{aligned} \quad (3)$$

Since the right-hand sides of Equations 1 and 3 are equal, the formulation of the ANSI standard based on Equation 1 is equivalent to stating that the threshold for a train of  $n$  pulses of pulsewidth  $t$  is equal to that for a single pulse of duration  $nt$ , independent of PRF or pulse train length.

In Table 4, this safety standard formulation (i.e., the empirical  $n^{3/4}$  model for multiple-pulse thresholds) is tested against the experimental data collected in this study and against the thermal model predictions. In this case, the thermal model predictions provide a significantly closer fit to the experimental data than those obtained from the empirical model. As shown in Figure 1, when the experimental data were entered on a log-log plot of threshold vs. number of pulses, an excellent fit to the data was found by a line with a slope of 0.91. The thermal model predictions also imply a straight line with a slope of 0.91, whereas the empirical model, by definition, yields a slope of 0.75.

TABLE 4. RELATIVE RETINAL THRESHOLDS FOR TRAINS OF 100-ms, 647-nm KRYPTON LASER PULSES(a)

$n$	Experimental data(b) $ED_{50}^0/ED_{50}^1$	Thermal model predictions $ED_{50}^0/ED_{50}^1$	Empirical model $ED_{50}^0/ED_{50}^1 = n^{3/4}$
1	1	1	1
2	1.7	1.8	1.7
5	-	4.2	3.3
10	7.6	7.9	5.6
50	34	35	19

(a) 200- $\mu$ m retinal image diameter, 6.25 Hz PRF

(b) From Table 2.

To exercise further both the thermal model and the tripartite comparisons of the preceding paragraph, we have examined the data of Ham et al. for trains of up to one million pulses from a laser scanning device (20). The wavelength is again 647 nm; the pulsewidth is 40  $\mu$ s; and PRF varies between four values: 100, 200, 400, and 1600 Hz. The log-log plot of threshold vs. number of pulses for Ham's data is shown in Figure 4. A least squares fit to the data yields a slope of 0.70, whereas the thermal model predictions which are also plotted on the figure are fit by a line with a slope of 0.92.

Summarizing the results of the two preceding paragraphs, we find that the thermal model predictions yielded a much closer fit to the experimental data generated in this study than did the empirical  $n^{3/4}$  model; but, when compared with the data of Ham et al. (20), the relative goodness of fit of the two models was almost exactly reversed. In both cases, the goodness of fit of either model seems acceptable relative to the experimental variability of the threshold data; and, at least for the ranges of exposure parameters examined here (where a thermal damage mechanism is thought to operate), we can feel quite comfortable in predicting multiple-pulse thresholds when the corresponding single-pulse threshold is known.

The following salient points are subject to the condition of a thermal damage mechanism being operative:

- 1) Additivity of multiple pulses is observed even for retinal image sizes as large as 500  $\mu$ m.

- 2) The repair or recovery of retinal tissue following sub-threshold laser exposures is slow, with a time constant of the order of several days. Therefore, the additivity of multiple pulses over any time frame up to, for example, 24 hr, is not affected by this repair process. Only when the effects of exposures repeated on a daily basis are of interest do we need consider modifying the predictive models to account for tissue repair processes.

- 3) Now that the validity of the thermal model has been established for multiple-pulse threshold predictions, the model can be exercised over broader ranges of exposure parameters for comparison to the empirical  $n^{3/4}$  model and to other available experimental data. Such calculations could be valuable in identifying conditions where the simple empirical predictor for multiple-pulse thresholds might produce poor results and compromise safety considerations. For example, preliminary thermal model calculations indicate a widening divergence with the empirical model as PRF appreciably exceeds 1 kHz (i.e., as interpulse intervals become short compared with the thermal relaxation rate). The high PRF regime is of significance to military operations, since a number of high PRF laser systems are already in use; so further thermal model calculations are in progress.

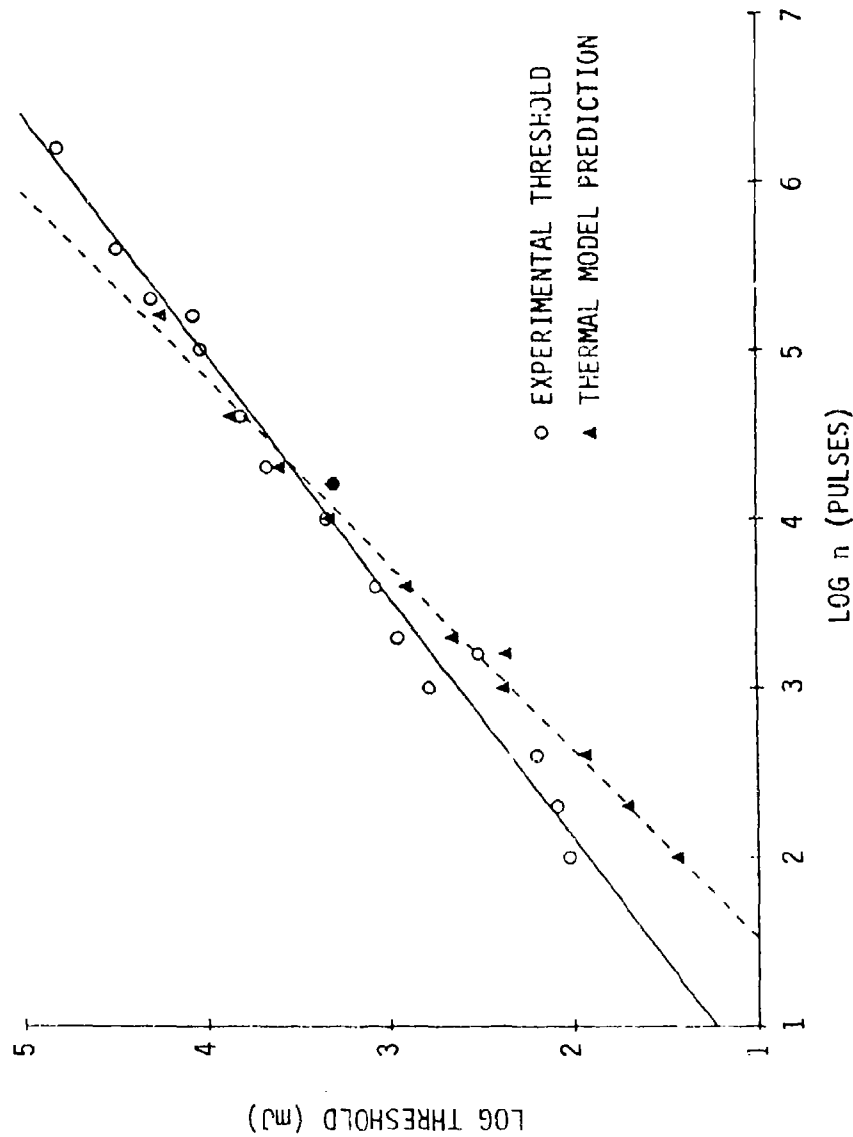


Figure 4. Log-log plot of threshold vs. number of pulses for 40- $\mu$ s, 647-nm krypton laser radiation at high PRFs (100-1600 Hz) (20). The best fit straight line to the experimental data (solid line) has a slope of 0.70. Thermal model predictions for the corresponding exposure parameters are also plotted ( $\Delta$ ), and fit by a line with a slope of 0.92 (dashed line).

## REFERENCES

1. Henriques, F.C. Studies of thermal injury. J Arch Pathol 43:489-502 (1947).
2. Moritz, A.R., and F.C. Henriques. Studies of thermal injury, II. Am J Pathol 23:695-720 (1947).
3. Mainster, M.A., T.J. White, J.H. Tins, and P.W. Wilson. Spectral dependence of retinal damage produced by intense light sources. J Opt Soc Am 60:848-855 (1970).
4. Takata, A.N., L. Goldfinch, J.K. Hinds, L.P. Kuan, N. Thomopoulos, and A. Weingandt. Thermal model of laser-induced eye damage. IITRI Tech Rep 74-6324, Final Report for Contract F41609-74-C-0005, USAF School of Aerospace Medicine, Oct 1974.
5. AFOSH Standard 161-10. Health hazards control for laser radiation. Dept. of the Air Force, Washington, D.C., 1980.
6. ANSI Standard Z136.1-1980. American national standard for the safe use of lasers. American National Standards Institute, Inc., New York, 1980.
7. ANSI Standard Z136.1-1986. American national standard for the safe use of lasers. American National Standards Institute, Inc., New York, 1986.
8. Stuck, B.E., D.J. Lund, and E.S. Beatrice. Repetitive pulse laser data and permissible exposure limits. Inst Rep No 58, Letterman Army Institute of Research, Presidio of San Francisco, CA, Apr 1978.
9. Griess, G.A., and M.F. Blankenstein. Multiple-pulse laser retinal damage thresholds. Am Ind Hyg Assoc J 42:287-292 (1981).
10. Zuclich, J.A., and J.S. Connolly. Ocular damage induced by near-ultraviolet laser radiation. Invest Ophthalmol 15:760-764 (1976).
11. Goldman, A.J., W.T. Ham, and H.A. Mueller. Mechanisms of retinal damage resulting from the exposure of rhesus monkeys to ultrashort laser pulses. Exp Eye Res 21:457-469 (1975).
12. Welch, A.J., L.A. Priebe, L.D. Forster, R. Gilbert, C. Lee, and P. Drake. Experimental validation of thermal retinal models of damage from laser radiation. USAFSAM-TR-79-9, Oct 1979.
13. Zuclich, J.A. Cumulative effects of near-UV induced corneal damage. Health Phys 38:833-838 (1980).
14. Griess, G.A., and M.F. Blankenstein. Additivity and repair of actinic retinal lesions. Invest Ophthalmol Vis Sci 20:803-807 (1981).

15. Finney, D.J. Probit analysis, 2nd ed. New York: Cambridge University Press, 1952.
16. Peaceman, D.W., and H.H. Rachford. The numerical solution of parabolic and elliptic differential equations. J Soc Indust Appl Math 3:28-41 (1955).
17. Mertz, A.R., B.R. Anderson, E.L. Bell, and D.E. Egbert. Retinal thermal model of laser-induced eye damage: computer program operator's manual. USAFSAM-TR-76-33, Nov 1986.
18. Gibbons, W.D., and R.G. Allen. Retinal damage from long-term exposure to laser radiation. Invest Ophthalmol Vis Sci 16:521-529 (1977).
19. Griess, G.A., M.F. Blankenstein, and G.G. Williford. Ocular damage from multiple-pulse laser exposures. Health Phys 39:921-927 (1980).
20. Ham, W.T., Jr., H.A. Mueller, J.J. Ruffolo, Jr., S.F. Cleary, R.K. Guerry, and D. Guerry, III. Biological applications and effects of optical masers. Final Report for Contract DAMD17-82-C-2083, U.S. Army Medical Research and Development Center, Apr 1987.